J. Phys. D: Appl. Phys. **34** (2001) 3209–3213 PII: S0022-3727(01)25977-4

Proximity correction simulations in ultra-high resolution x-ray lithography

A J Bourdillon[1] **and C B Boothroyd**[2]

[1] P O Box 641385, San Jose, CA 95164, USA
[2] Department of Materials Science and Metallurgy, Pembroke Street, Cambridge CB2 3QZ, UK

Received 21 June 2001
Published 6 November 2001
Online at stacks.iop.org/JPhysD/34/3209

Abstract
This paper follows previous demonstrations of demagnification by bias in ultra-high resolution proximity x-ray lithography. The demagnification, $\times 1$–$\times 6$, is achieved without lenses or mirrors. Two-dimensional proximity corrections, applied to rectangular mask shapes, are simulated. A V-shaped inrigger, cut into the mask, is particularly effective. When a typical range of broadband illumination wavelengths is used, several beneficial effects are observed when the gap is held at the 'critical condition'. Maintaining fine resolution, oscillations—due to Fresnel diffraction parallel to the longer dimension of a rectangle—are virtually eliminated, and the image intensity is made uniform by the elimination of bright spots near the ends of a rectangle.

1. Introduction

Prints with 20 nm feature size have been demonstrated [1–3] by proximity x-ray lithography (PXL). Typical 1–2 kV incident beam energies (1.2–0.6 nm wavelengths) were used and demagnification up to 9×—through two-sided bias, without lenses or mirrors—was obtained with correspondingly large mask feature sizes and comparatively large mask−wafer gaps. The technique, called ultra-high resolution lithography (UHRL), which uses Fresnel diffraction positively near a 'critical condition' (CC) (see below and [1]) results in demagnification by bias. The demagnification is not generally uniform because the bias is more or less constant around the edge of the image so that the bias is subtracted from the size of the mask aperture when the print is developed. The demagnification has considerable importance in a wide range of applications including integrated circuit manufacture [4] and manufacture of micro electromechanical systems.

Thus PXL, which is the most consistently demonstrated of the next generation lithographies [5–9], is extensible beyond previously supposed limits. Typically synchrotron radiation is used and this is naturally collimated by relativity so that the penumbra is controlled to within one nanometre. To provide uniform illumination, the x-ray beam is typically scanned, off an oscillating grazing-incidence mirror, across the mask−wafer system. Exposures of full fields, typically 50 × 30 mm, are made in a time of about 1 s. The mask is held stationary while the wafer is stepped and aligned between exposures on different fields.

Previously we have reported the results of simulations [1] which have shown the effects of (a) varying the mask–wafer gap about the critical condition, (b) the distortion observed in non-symmetric features, and (c) high frequency ringing parallel to longer dimensions. The simulations have been performed for both monochromatic incident radiation and for the wide band of wavelengths typically used in PXL. Significantly, in the latter case, the ringing is virtually eliminated. The chief residual effect is a bright spot produced near the ends of, for example, rectangular images (as below). The bright spot corresponds to the maximum peak well known in Fresnel diffraction from a knife-edge. We have also simulated the effects of outriggers on mask imaging and observed changes in intensity. We noticed that the ringing results from Fresnel diffraction from the larger dimensions [1] when the smaller dimensions are held close to critical. The simulations have been generally verified in experimental demonstrations [1–4]. Here we examine how the bright spot can be reduced by inriggers, i.e. deviations sectioned from a simple mask pattern (below). The importance of this bright spot results from the modern process control used in the development of resists. The controlled selection of development level is an important parameter in setting the demagnified feature size reduction. Though the bright spots ensure local development, i.e. above a selected level at lower intensity, an inability to control them will limit the shapes, including corners, that can be developed.

As is illustrated in figure 1, which represents parallel illumination passing through a clear mask feature forming an

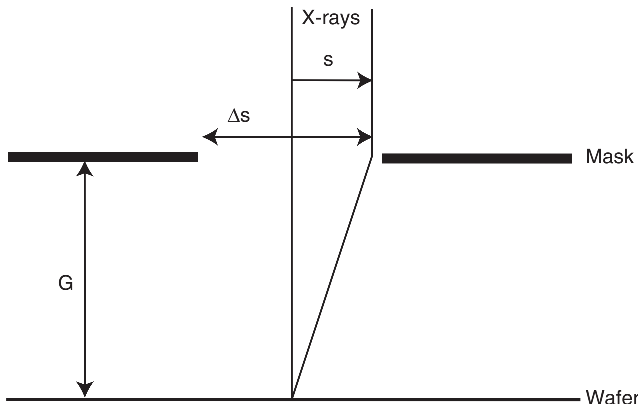

Figure 1. Two rays from a distant synchrotron radiation source passing through a clear transmitting mask feature of width Δs, construct an image at the axial point A, on the plane of the wafer. The off-axis ray suffers a phase lag proportional to $2\pi s^2\lambda^{-1}$ whose phase is represented on the Cornu spiral (see [1]), and where λ is the wavelength of the radiation.

image on some plane at gap G, a ray off-axis suffers a phase shift $2\pi s^2/\lambda$ relative to the axial ray, where s is the distance off-axis and λ is the wavelength of the illumination. The CC is defined, as follows, in terms of the dimensionless spatial coordinate, v [10], as applied to the case with parallel incident illumination [1], where

$$v = s\sqrt{\frac{2}{G\lambda}} = \sqrt{2\tilde{N}_{\mathrm{F}}} \qquad (1)$$

and $\tilde{N}_{\mathrm{F}}$ is the number of Fresnel (half wavelength) zones.

For a one-dimensional line feature, the construction of wave amplitudes at the image plane (on the wafer) can be represented by means of the well-known Cornu spiral [10], the phases of individual rays being represented by infinitesimal arrows lying on the spiral. When the size of a clear mask feature Δv is equal to 2.42, the wave amplitude at the wafer on the axis of the mask feature is maximum [1] and the aerial image sharpest. This is the 'critical condition' and for a given s and λ , the CC depends on G. The clear mask feature then covers just less than two and a half Fresnel half zones. For various values of print feature size and selected demagnification, the corresponding mask feature size and critical gap, G_{c}, are shown in table 1. The demagnification depends on the exposure and development levels and, with controlled processing, can be readily selected over the range $\times 1$–$\times 6$. It turns out that the CC is actually critical in second order since there remains a wide latitude in gap spacing for a required print resolution.

To understand the independent effects of mask feature shape, wavelength and gap for the two-dimensional images, idealized simulations were performed for the intensities below the mask. A routine was used which is based on the multislice method written in the Semper [11] image processing program. This routine allows the Fresnel diffraction from arbitrarily shaped masks in one or two dimensions to be calculated at any distance from the mask.

For ease of understanding, opaque masks were used in these simulations. Previously we have investigated masks with a typical transmittance of 80% in the opaque regions [1].

Table 1. At the critical condition ($\Delta v = 2.42$) and wavelength $\lambda = 1$ nm, the gap is given by $G_{\mathrm{c}} = (\Delta s)^2/2.9$. For selected demagnifications and print feature sizes this critical gap, G_{c}, is tabulated.

Demagnification	Print feature size (nm)	Mask feature size Δ (μm)	Mask-wafer gap G_{c} (μm)
×2	100	200	14
	75	150	8
	50	100	4
	25	50	1
×3	100	300	31
	75	225	18
	50	150	8
	25	75	2
×4	100	400	55
	75	300	31
	50	200	8
	25	100	4
×5	100	500	86
	75	375	49
	50	250	22
	25	100	4
×6	100	600	124
	75	450	70
	50	300	31
	25	150	8

The chief effects of this residual transmittance were shown to lie in the side bands which are reduced to insignificance in UHRL since the side bands have low intensity and do not affect resolution at the high development levels employed here (cf prior art 1 : 1 proximity printing as in [8]). Our masks [1–3] were made by standard procedures [6–8] on standard fixtures, and used a gold absorber on a transmitting SiN substrate. Tantalum compound absorbers on SiC substrates are known to be more robust but not necessary for the experiments earlier performed.

Figure 2(*a*) shows a rectangular aperture representing $150 \times 600\,\mathrm{nm}^2$ dimensions. In figure 2(*b*), the simulated image was produced by monochromatic 0.8 nm wavelength x-rays with a mask–wafer gap of 9.8 μm ($\Delta v = 2.4$). In UHRL the (two-sided) bias is constant and this leads to distortions when the clear mask feature is not symmetric (circular or square). The distortion can be readily compensated at the mask-writing stage but there exists a second effect when the gap is held critical for the shorter dimension to enhance the resolution at printing. There is a ringing parallel to the longer dimension similar to the oscillations observed in well-known Fresnel diffraction from a knife-edge [10]. Moreover a bright spot can be seen towards the ends corresponding to the maximum in the Fresnel knife-edge pattern. With monochromatic incident radiation, the ringing is unavoidable because the gap cannot be held at the CC for both dimensions at the same time. Away from the CC, e.g. at a gap of 30 μm ($\Delta v = 1.4$ as in figure 2(*c*)), the image pattern broadens and there are some changes in the ringing with bright regions still exhibited near the ends. When broad spectrum incident radiation is used, e.g. in the range 1–2 kV (0.62–1.24 nm; $2.7 < v < 1.9$), three important effects occur. These are shown in figure 2(*d*). Firstly, the resolution is hardly degraded, secondly the ringing is virtually eliminated except that, thirdly, the bright spots remain near the ends of the image fields. Away from the

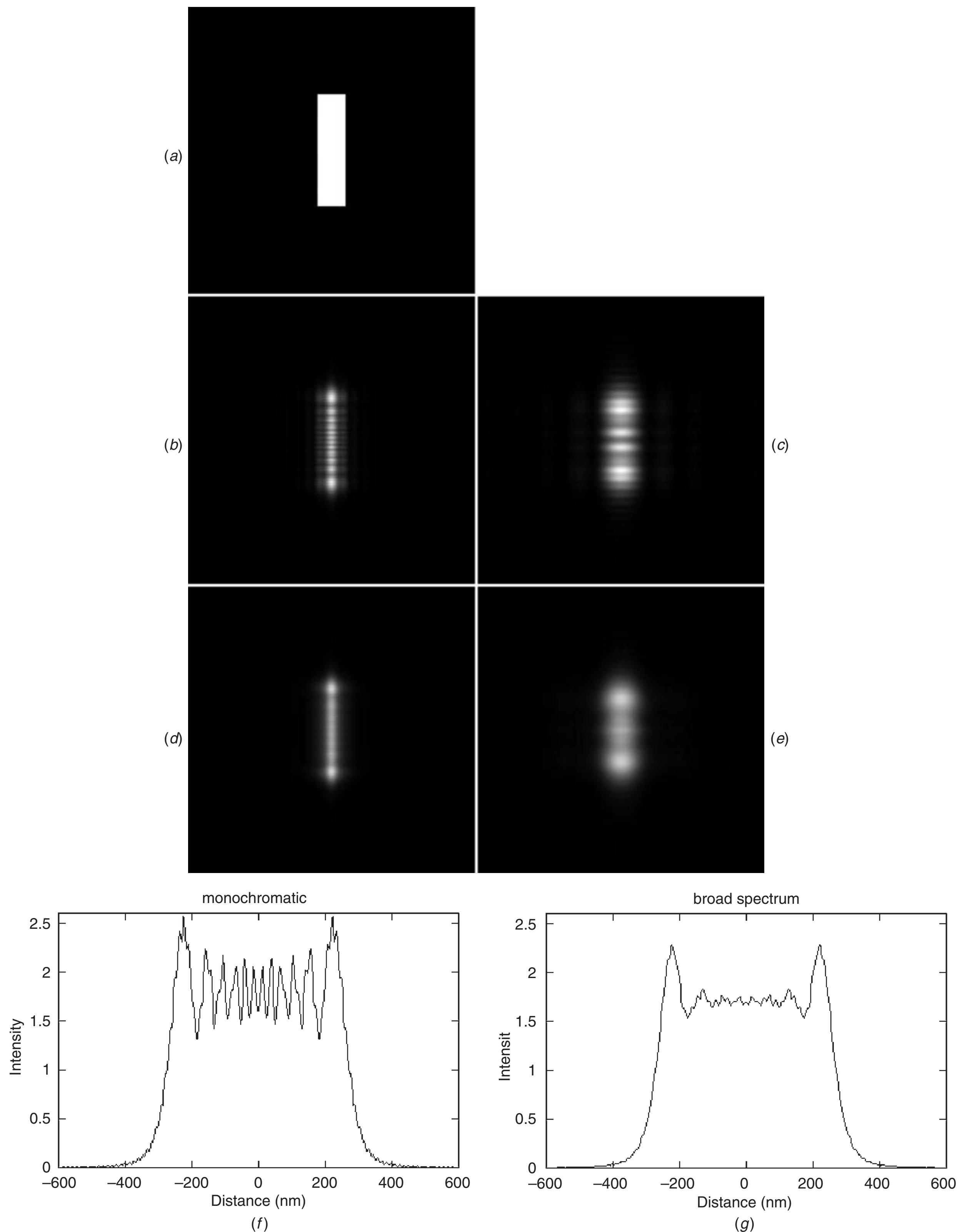

Figure 2. (*a*) Two-dimensional rectangular mask slit of size $150 \times 600\,\text{nm}^2$ with intensity scale white=1; (*b*) simulated image due to 0.8 nm x-rays transmitted at a distance of 9.8 µm through the clear mask feature behind the otherwise opaque mask, i.e. for the critical $\Delta\nu = 2.4$ and intensity scale white = 2.7; (*c*) simulated image due to 0.8 nm x-rays transmitted at a distance of 30 µm behind the opaque mask and aperture, with $\Delta\nu = 1.4$. Notice that the ripple in the image intensity due to the longer dimension and bright fringes at ends are both significantly reduced in (*d*), simulated under the same conditions but using a flat bandpass ranging over $0.62 < \lambda < 1.28\,\text{nm}$ (corresponding to $1.9 < \nu < 2.7$) and intensity scale white = 1.33. Notice that when the mean $\langle \Delta v \rangle$ differs from critical, the image resolution (*e*) reverts towards 1(*c*), i.e. resolution is lost; though the ripples are greatly reduced and the bright spots remain. The figure in (*f*) shows the intensity profile down the centre of figure (*b*) and figure (*g*) shows the profile down the centre of figure (*d*), i.e. using broadband.

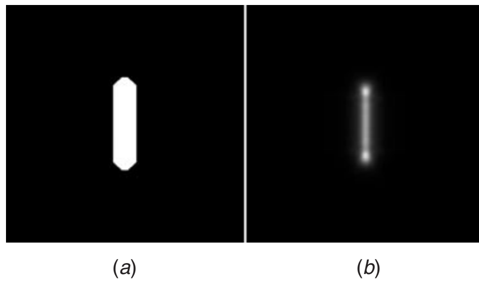

Figure 3. (*a*) Two-dimensional rectangular mask slit of size 150 × 600 nm^2 as in figure 2 but with chopped-off corners. (*b*) Simulated under corresponding conditions as in figure 2(*d*). The comparison shows that the ripple is reduced by the chopped-off corners, though the bright spots near the extremities remain.

CC (figure 2(*e*)), the bright spots remain together with print feature broadening and also a reduction of ringing. Further details of these simulated images are illustrated with intensity profiles. Figure 2(*f*) shows the intensity profile of the aerial image (figure 2(*b*)) parallel to the long axis of the aperture, with monochromatic radiation; while figure 2(*g*) shows the same for figure 2(*d*).

With figures 2(*a*)–(*f*) as a reference, several simulations were performed using various inriggers. Two examples are given here. In figure 3 proximity corrections in the form of a rectangular pattern with lopped-off corners are simulated. The conditions simulated are, except for the inrigger, the same as those corresponding to figure 2. The results are generally consistent but with a significant general reduction

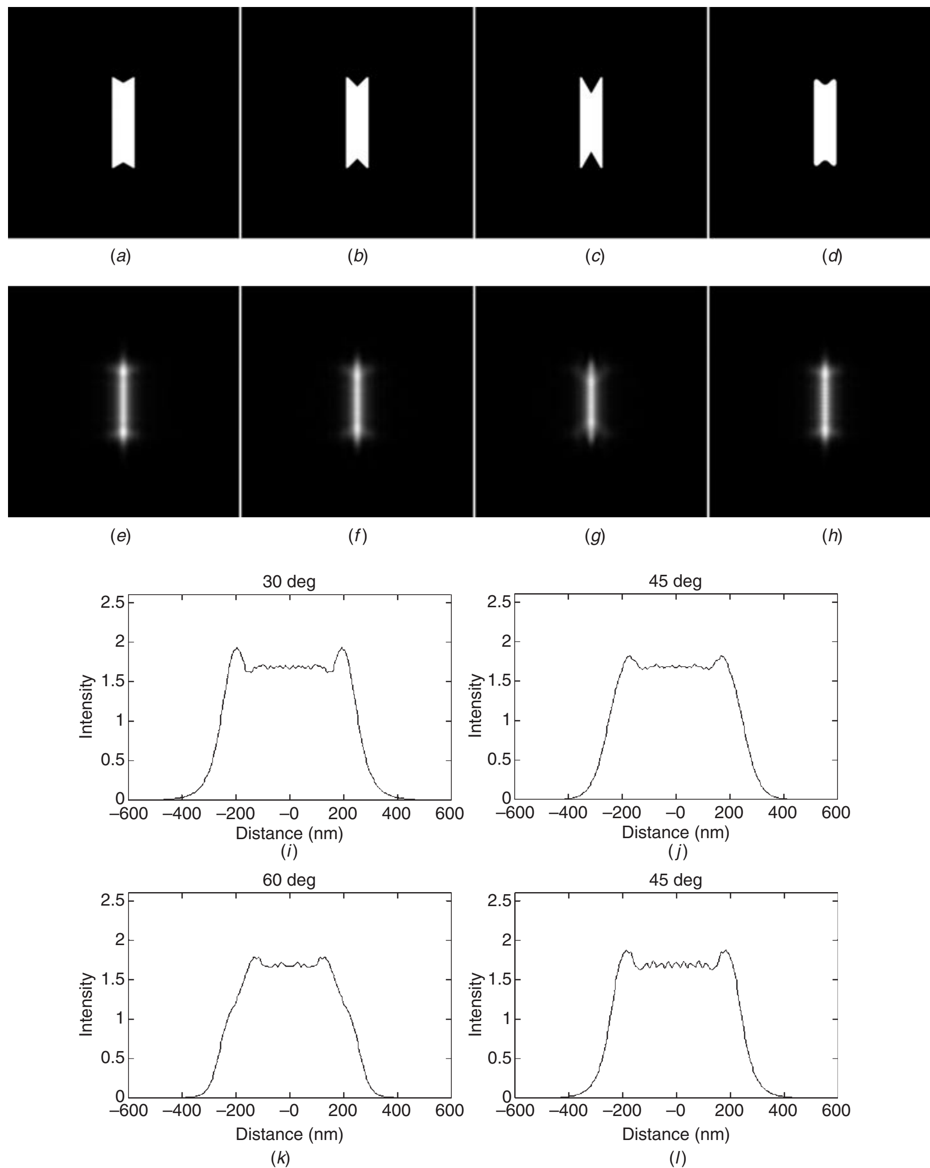

Figure 4. (*a*) Two-dimensional rectangular mask slit of size 150 × 600 nm^2 as in figure 2(*a*) but with V-shaped inrigger at angle 30° (*b*) same but with angle 45° (*c*) same but with angle 60°; and (*d*) same with blurred angle about 45° as shown. Corresponding simulations, (*e*)–(*h*), are shown using the same conditions as figure 2(*d*), i.e. with broadband 1–2 kV incident radiation. (*i*) Intensity profile down the vertical axis of (*e*); (*j*)–(*l*) corresponding profiles for (*f*)–(*h*).

in ringing due to the broken edge at the extremities of the aperture in figure 3. However, the bright spots near the ends remain and seem to be enhanced when compared with corresponding spots from the untrimmed rectangular aperture (figure 2(*d*)).

Figures 4(*a*)–(*d*) show four apertures similar to that shown in figure 2(*a*) but with V-shaped inriggers having angles of 30° , 45° (unblurred), 60° and 45° (blurred). Corresponding simulations are shown in figures 4(*e*)–(*h*) and profiles in figures 4(*i*)–(*l*). In these simulations, broadband 1–2 kV incident radiation is used. The V-shaped inriggers systematically reduce the height of the bright spots, the reduction increasing with decreasing angle. The reduction in spot height is accompanied by a systematic reduction in slope at the image edges and by lesser changes in ripple. Since a steep slope leads to improved process control during resist development, a compromise is sought. With a blurred 45 (figure 4(*l*)), the slope is sharpened without significant increase in bright spot height. Thus the blurred (or rounded) V shows the best promise for providing uniform illumination with sharp aerial images. Significantly, the simulated image in figure 4(*l*) shows that both the bright spots and ripple are virtually eliminated when the blurred 45° V-shaped inrigger is applied.

In conclusion, a proximity correction has been shown, by simulation, to provide uniform illumination from a two-dimensional mask in ultra-high resolution proximity x-ray lithography and the way has been demonstrated for optimization of the image for the specific demands of particular applications. The simulations are generally consistent with experimental results on prints of dimension down to 20 nm. The simulations demonstrate the practicality of control of print shaping by the use of inriggers and provide a solution to the occurrence of bright spots in two-dimensional simulations.

References

[1] Bourdillon A J, Boothroyd C B, Kong J R and Vladimirsky Y 2000 *J. Phys. D: Appl. Phys.* **33** 1–9

[2] Vladimirsky Y, Bourdillon A J, Vladimirsky O, Jiang W and Leonard Q 1999 *J. Phys. D: Appl. Phys.* **32** L114–L118

[3] Kong J R, Vladimirsky Y and Quinn L *Proc. MNE 2000* (*Jena, Sept. 18–21*), Germany

[4] *Solid State Technology* February 2000, News Item, pp 18–23

[5] Neureuther A R Microlithography with soft x-rays *Synchrotron Radiation Research* ed H Winich and S Doniach (New York: Plenum)

[6] Vladimirsky Y 1998 Lithography *Vacuum Ultraviolet Spectroscopy II* ed J A Samson and D L Ederer (*Experimental Methods in the Physical Sciences*) 32 (New York: Academic) pp 205–223

[7] Cerrina F 1997 X-ray lithography *Handbook of Microlithography, Micromachining, and Microfabrication* vol **1**, ed P Rai-Choudhury (Bellingham, Washington: SPIE) pp 253–319

[8] Krasnoperova A A, Rippstein R, Flamholz A, Kratchmer E, Wind S, Brooks C and Lercel M, 1999 *Proc. SPIE* **3676** 24–39

[9] Vladimirsky Y 1999 Introduction: limits or limitations *Proc. SPIE* **3676** xvi–xvii

[10] Jenkins F A and White H E 1957 *Fundamentals of Optics* (New York: McGraw-Hill)

[11] Saxton W O, Pitt T J and Horner M 1979 *Ultramicroscopy* **4** 343